

1 **Unraveling the Molecular Basis of Substrate Specificity and Halogen Activation**
2 **in Vanadium-Dependent Haloperoxidases**

3 P. Zeides,^{a,b} K. Bellmann-Sickert,^b Ru Zhang,^b C. J. Seel,^a V. Most,^c C. T. Schoeder,^c M.
4 Groll,^d T. Gulder^{a,b,e,f*}

5 ^aBiomimetic Catalysis, Catalysis Research Center, TUM School of Natural Sciences,
6 Technical University of Munich, Lichtenbergstrasse 4, 85748 Garching, Germany

7 ^bInstitute of Organic Chemistry, Faculty of Chemistry and Mineralogy, Leipzig University,
8 Johannisallee 29, 04103 Leipzig, Germany

9 ^cInstitute for Drug Discovery, Leipzig University, Faculty of Medicine, Liebigstr. 19, 04103
10 Leipzig

11 ^dDepartment of Bioscience, Center for Protein Assemblies, TUM School of Natural Sciences,
12 Technical University of Munich, Ernst-Otto-Fischer Strasse 8, 85748 Garching, Germany

13 ^eInstitute of Organic Chemistry, Campus C4.2, Saarland University, 66123 Saarbruecken,
14 Germany

15 ^fSynthesis of Natural-Product Derived Drugs Group, Helmholtz Institute for Pharmaceutical
16 Research Saarland (HIPS), Helmholtz Centre for Infection Research (HZI), Campus E8.1,
17 66123 Saarbrücken, Germany

18 e-mail: tanja.gulder@uni-leipzig.de

19 **Abstract**

20 Vanadium-dependent haloperoxidases (VHPOs) are biotechnologically valuable and
21 operationally versatile biocatalysts that do not require complex electron shuttling systems.
22 These enzymes share remarkable active-site structural similarities yet display broadly variable
23 reactivity and selectivity. The factors dictating substrate and halogen specificity and, thus, a
24 general understanding of VHPO reaction control still need to be discovered. This work's
25 strategic single-point mutation in the cyanobacterial bromoperoxidase *Am*VHPO facilitates a
26 selectivity switch to allow aryl chlorination. This mutation induces loop formation absent in the
27 wild-type enzyme, and that interacts with the neighboring protein monomer, creating a tunnel
28 to the active sites. Structural analysis of the substrate-R425S-mutant complex reveals a
29 substrate-binding site at the interface of two adjacent units. There, residues Glu139 and
30 Phe401 interact with arenes, extending the substrate residence time close to the vanadate
31 cofactor and stabilizing intermediates. Our findings validate the long-debated existence of
32 direct substrate binding and provide detailed VHPO mechanistic understanding. This work will
33 thus pave the way for a broader application of VHPOs in diverse chemical processes.

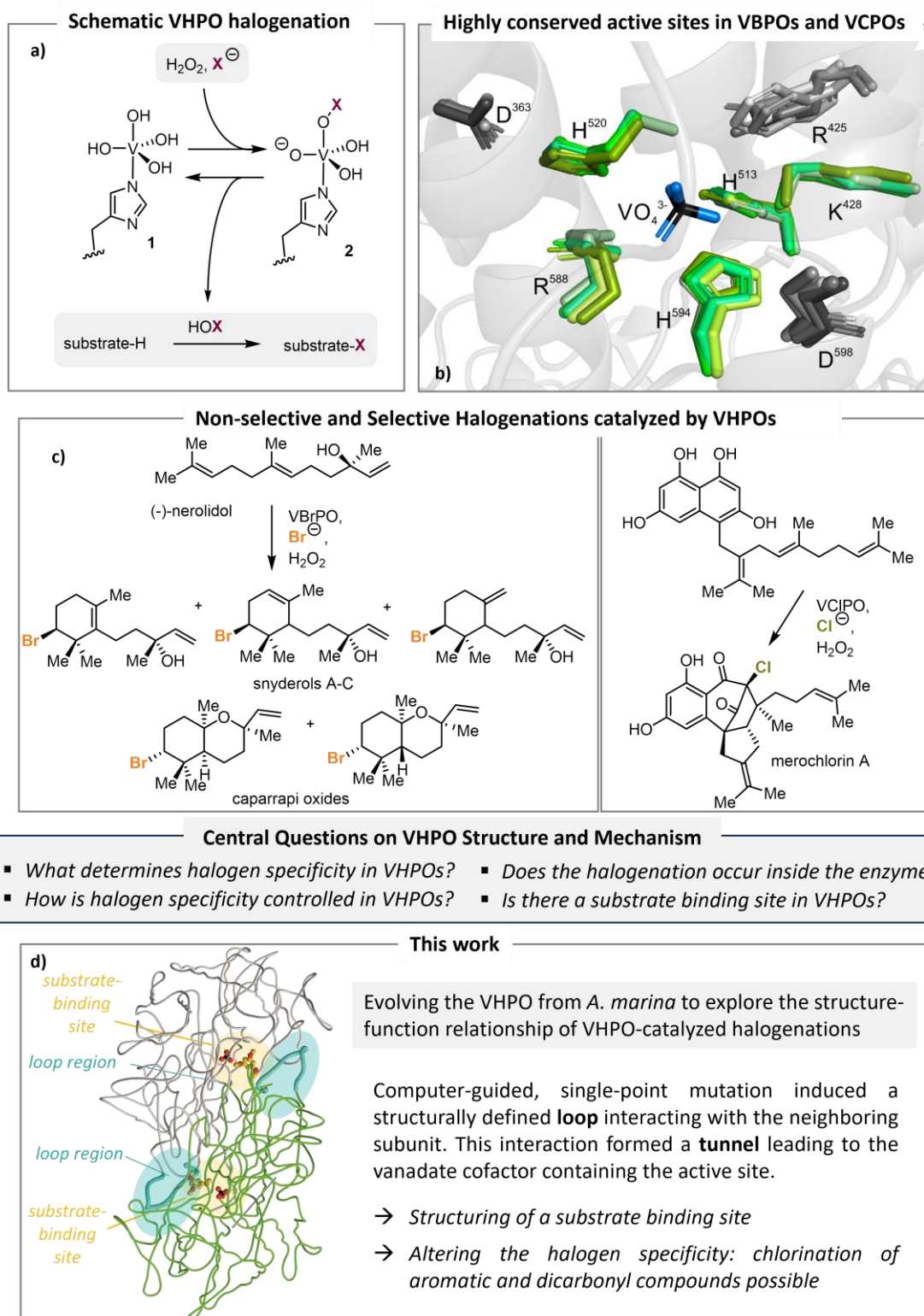
35 Introduction

36 Halogenation plays a crucial role in molecule construction and manufacturing, as halogenated
37 compounds are found in almost all areas of our society, ranging from solvents, refrigerants,
38 propellants, plastics, pesticides to drugs. For example, in annual sales of the 100 most popular
39 pharmaceuticals, 13% of active pharmaceutical ingredients (APIs) contain chlorine or bromine.
40 Even more impressive, 63% of these blockbuster drugs require a halogenation step within their
41 manufacturing process.¹ The broad versatility of organohalides stems from their high reactivity
42 and chemical orthogonality, allowing for various selective transformations, particularly cross-
43 coupling and substitution chemistry. Generating organohalides still mainly involves adding
44 corrosive molecular halogens in combination with metal catalysts or electrophilic
45 organohalogen reagents that enable nucleophilic substitution (S_N2) or electrophilic aromatic
46 substitution (S_EAr).² However, these reactions pose challenges regarding their environmental
47 impact, sustainability, and selectivity, mainly due to the toxic, corrosive, and non-atom
48 economic nature of the reagents employed and their tendency to produce complex product
49 mixtures. Although recent achievements in homogeneous catalyst development have led to
50 more selective catalytic halogenation approaches, these catalysts tend to be intricate,
51 expensive, and time-consuming to synthesize.

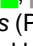

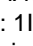


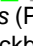

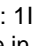

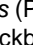
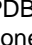
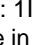

52 In contrast, nature has evolved different strategies to create C,X-bonds precisely under mild
53 conditions, as evidenced by ca. 5000 halogenated natural products isolated to date.³ The most
54 common strategy in nature is electrophilic halogenation⁴ facilitated by vanadium- (VHPOs) and
55 heme-dependent haloperoxidases, and flavin-dependent halogenases. VHPOs exhibit an
56 attractive biotechnological potential for industrial applications⁵ because of their unusually high
57 stability, high tolerance to synthetic reaction conditions, such as organic solvents, and their
58 broad substrate range.⁶ In addition, they are capable of oxidizing halides (I⁻, Br⁻, Cl⁻) in the
59 presence of hydrogen peroxide rather than utilizing complicated electron delivery chains, e.g.,
60 via nicotinamide cofactors.⁷ VHPOs are categorized according to the most electronegative
61 halide they can oxidize, leading to chloroperoxidases (VCPOs), bromoperoxidases (VBPOs),
62 and iodoperoxidases (VIPOs). The general mechanism for VHPO-catalyzed reactions is based
63 on the two-electron oxidation of halides.^{4a,8} Theoretical and experimental studies propose that
64 this process starts with hydrogen peroxide coordinating to the vanadium(V) center in **1**, forming
65 a peroxy-vanadate complex. Subsequent attack of a halide ion at the partially positively
66 charged oxygen atom in **2** leads to an electrophilic halogen species, most likely in the form of
67 diffusible hypohalous acid (HOX), which reacts with a suitable substrate.^{4a} The vanadium(V)
68 oxidation state is retained in the catalytic cycle. Therefore, the metal cofactor remains redox-
69 neutral, and consequently, no regeneration is required. The existence of a binding site for

70 organic molecules to be halogenated in VHPOs is controversially discussed.⁹ In several
71 reports, a substrate binding site for organic substrates has been proposed⁹⁻¹⁰ because of the
72 low halogenation reactivity of HOX in solution and the selective halogen delivery catalyzed by
73 VCPOs from *Streptomyces* bacteria,¹¹ but its existence has yet to be proven.

74 Overlays of X-ray structures of VBPOs from different species (from *A. marina*, *C. pilulifera*, *C.*
75 *officinalis*, and *A. nodosum*) with the VCPO from *C. inaequalis* revealed that the key catalytic
76 residues in the active site are superimposable despite overall low sequence similarity between
77 VBPOs and VCPOs (e.g., *An*VHPO vs *Ci*VHPO; 21.5% sequence identity, see SI,
78 SFig. 21).^{6d,12} In all VHPOs known so far, the vanadate anion is bound to an axial histidine and
79 further stabilized by hydrogen bonding interactions with the protein backbone. The amino acids
80 involved in vanadate coordination and cofactor binding are conserved in position and
81 orientation in this class of enzymes. Nevertheless, VHPOs differ in their oxidizing power. The
82 halogen specificity is thus due to structural changes in an outer sphere surrounding the active
83 center. Despite intense mechanistic and structural studies, especially on HOX generation,
84 essential halide, and substrate specificity questions remain unresolved.



85

86 **Fig. 1 | Central questions on VHPO mechanism.** a) Schematic representation of the mechanism of the VHPO-
 87 catalyzed halogenation. b) Structure alignment of active site residues (green) and residues proximal to the active
 88 site (grey) of selected vanadium-dependent haloperoxidases from *A. marina* (PDB: 5LPC, , , , , , *A. nodosum* (PDB:
 89 1QI9, , , *C. officinalis* (PDB: 1QHB, , , *C. pulifera* (PDB: 1UP8, , , *C. inaequalis* (PDB: 1IDQ, , ). The
 90 residue nomenclature follows the sequence of the bromoperoxidase of *A. marina*. The backbone in grey is derived
 91 from the crystal structure of *A. marina* (PDB: 5LPC). c) Selected example of a non-selective and a selective
 92 halogenation catalyzed by algal VHPOs¹³ and *Streptomyces CNH-189*, respectively.^{11e} d) This work delivering
 93 molecular insights gained by single point mutations of R425 and the structure-activity analysis of this mutant.

94

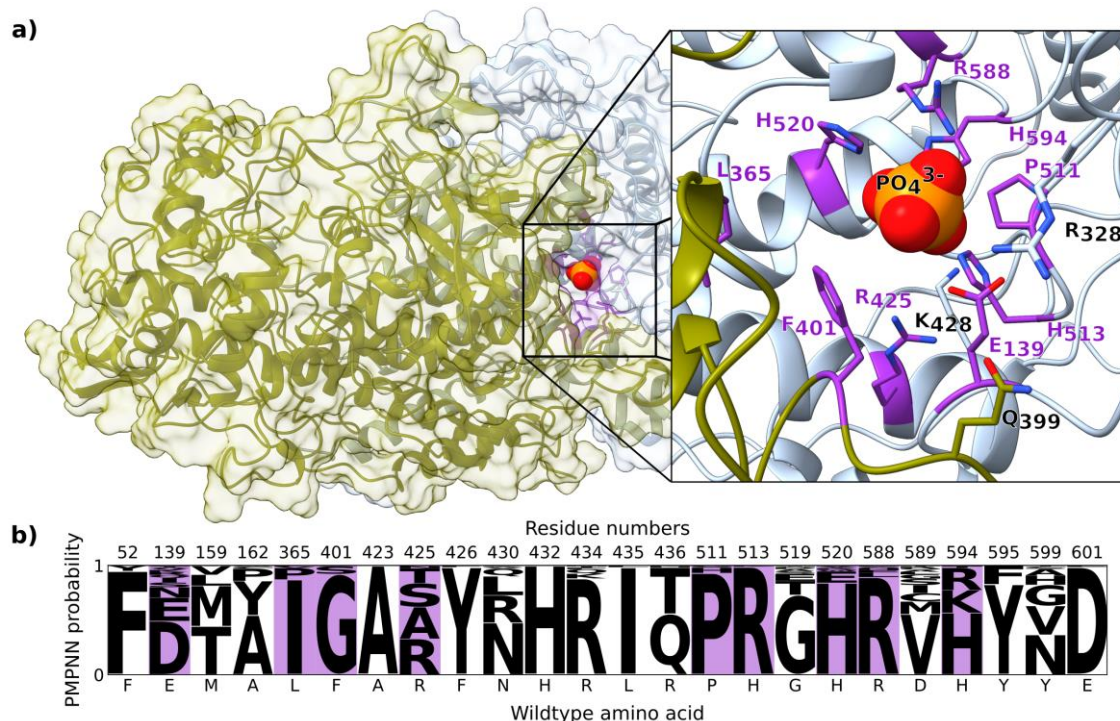
95 Here, we set out to decipher the structural factors determining halogen specificity in VHPOs.
96 Using computer-assisted protein design,¹⁴ sampled mutations allowing for sequence variability
97 to influence chlorination rate while maintaining structural integrity and stability were predicted
98 in the cyanobacterial VBPO from *Acaryochloris marina*. The Arg at position 425, located
99 outside the active site, stood out as being replaceable with smaller and polar amino acids,
100 such as Ser (R425S). Mutagenesis experiments in the second shell combined with activity
101 screening assays revealed that R425S-VCPO was transformed into a chloroperoxidase
102 capable of efficient aromatic chlorination, even on a preparative scale. Subsequent X-ray
103 crystal structure analysis of the R425S variant visualized the formation of structural elements
104 (residues 390-404) that are intrinsically distorted in wild-type *Am*VHPO. Intriguingly, the
105 structural motif is only involved in intermolecular interactions with the active site of the
106 neighboring subunit. There, it introduces a tunnel to the catalytic metal center and, at the same
107 time, forms a precise binding site ideal for aromatic substrates. Thus, the combined
108 computational, structural, and chemical approach revealed that the halogen specificity is
109 coordinated at the intersection of subunits, and an induced fit mechanism for substrate binding
110 is proven by co-crystallization experiments of trimethoxybenzene (**7**) with the R425S-VCPO.
111 In summary, the validated substrate binding channel and the halogen specificity are significant
112 observations for enzyme engineering and database-driven predictions of VCPO-enzyme
113 functions.

114

115 **Computational screening for mutation sites close to the vanadate binding site.** For
116 elucidating the halogen specificity in VHPOs, we chose the vanadium-dependent
117 haloperoxidase *Am*VHPO from the cyanobacterium *Acaryochloris marina* MBIC 11017.^{6d}
118 *Am*VHPO is available in high yields (30 mg L⁻¹) using a recombinant *E. coli* expression system
119 and is structurally well characterized. In addition, the enzyme shows remarkable robustness
120 towards organic solvents and heat, together with a broad substrate scope for aromatic
121 bromination, making it a perfect candidate for mechanistic investigations and biotechnological
122 applications.^{6d,7,13b,15} We started our studies by identifying amino acids near the active site that
123 can be modified without affecting the expression of the enzyme (Fig. 2a). Using a model of the
124 *Am*VHPO structure (cf. SI, SFig. 13 and 14), we designed the sequence using the deep
125 learning-based method ProteinMPNN.¹⁶ Interestingly, position R425 was predicted to respond
126 well to substitutions with smaller amino acids, such as Ala or Ser (Fig. 2b). Notably, this
127 arginine residue is located i-3 from the active site lysine (i-3K, Lys428 *Am*VHPO, see SI, SFig.
128 13b). While the sequence alignment with other VHPOs revealed R425 in VBPOs from the red
129 algae *Corallina officinalis* and *C. pilulifera*, chlorinating VHPOs from the fungus *Curvularia*
130 *inaequalis* and the brown alga *Ascophyllum nodosum* consist of a Trp in these positions (Fig
131 1b). Indeed, Izumi *et al.*¹⁷ showed that a mutation of R397 in *Cp*VHPO (corresponds to R425

132 in *Am*VHPO) to Phe or Trp increased chlorination activity. Additional calculations using the
133 cartesian $\Delta\Delta G$ protocol implemented in Rosetta¹⁸ revealed that substitutions of R425 by small
134 side chains do not confer an energetic advantage. However, these mutations increase solvent
135 accessibility at the enzymatic site (see SI, SFig. 13c and 16).

136



137

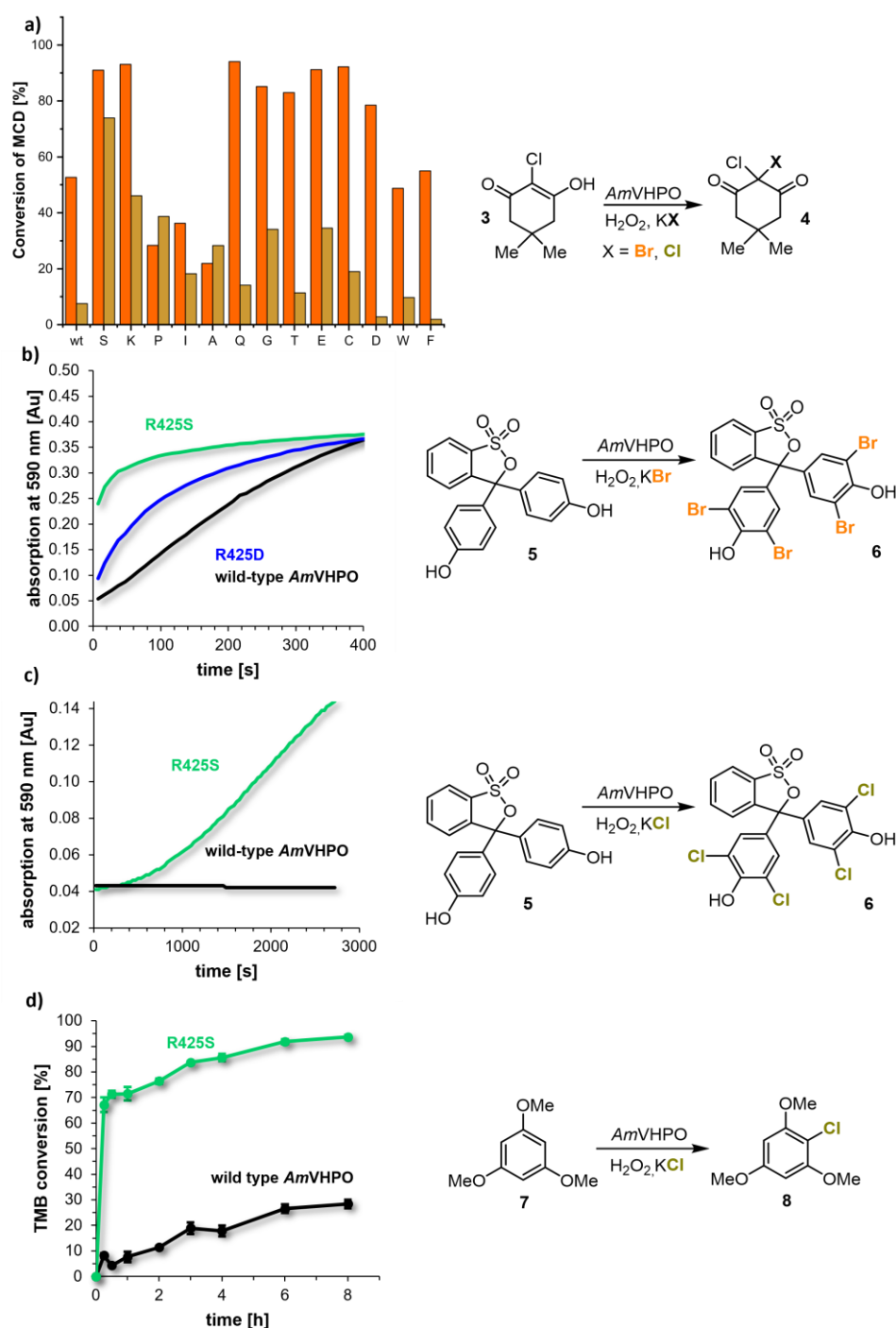
138 **Fig. 2 | Sequence design of residues in proximity to the active site.** a) Visualization of the *Am*VHPO model.
139 Two chains of the decamer are shown. The design of surface-exposed residues was simulated in a 10 Å radius of
140 the catalytic residue K428. Designed residues pointing towards the substrate channel are highlighted in violet. The
141 phosphate position was superimposed from 5LPC.^{6d} b) Conditional probabilities predicted by ProteinMPNN¹⁶
142 for the designed positions in the *Am*VHPO dodecamer model.

143

144 **Changing *Am*VHPO reactivity by mutagenesis at R425.** We created a library of mutant
145 enzymes by site-saturated mutagenesis of the targeted R425 to validate the calculated results
146 and screened the catalytic fidelity of the obtained mutants using the UV monochlorodimedone
147 (MCD, **3**) assay.¹⁹ The results clearly showed that position 425 is critical for the substrate
148 specificity of *Am*VHPO (see SI, chapter 3). Strikingly, the reaction rate of bromination and
149 chlorination drastically increased from 53% for bromination and 8% for chlorination for the wild-
150 type *Am*VHPO to 91% and 74%, respectively, for the R425S variant (Fig. 3 and SI). The
151 exchange of R425 by Ala (21% bromination of **3**; 28% chlorination of **3**) and Thr (83%
152 bromination of **3**; 11% chlorination of **3**), which were both likewise predicted by ProteinMPNN
153 (cf. Fig. 2), also showed an overall enhanced halogenation activity compared to the wild-type,

154 but this was not as significant in terms of chlorination as observed for the R425S mutant.
155 Interestingly, substituting R425 with either Phe (2% chlorination of **3**) or Trp (10% chlorination
156 of **3**) displayed almost no change or even a decrease in chlorination activity.

157 Enzyme kinetics for chloride, bromide (see SI, chapter 5), and hydrogen peroxide as substrates
158 were determined using the MCD assay with saturating levels of the respective remaining
159 substrates at the optimum pH value (pH 6.0) to classify the reaction as pseudo-first order.
160 Kinetic parameters for chloride and H₂O₂ were determined based on Michaelis-Menten curves.
161 The K_M values for H₂O₂ were similar between the R425S mutant (66 μM) and the wild-type (60
162 μM),^{6d} while the binding constants for chloride differed significantly. Only for the mutant it was
163 possible to determine the K_M for chloride, leading to 167 mM, which is in line with that of other
164 VHPOs showing significant chlorinating ability, such as the *An*VHPO (344 mM) from brown
165 algal¹⁷ or the VCPO from the deep-sea hydrothermal vent fungus *Hortaea werneckii* (237
166 mM).²⁰ Taken together, the change of the i+3 amino acid did not affect the binding of the
167 oxidant H₂O₂ to the enzyme's active site but dramatically affected chloride processing. As
168 different amino acids three positions apart from the active site lysine (Lys428) trigger an
169 enhanced chlorination activity in different VHPOs, such as, e.g., Phe and Trp in *Cp*VHPO, Trp
170 in *An*VHPO or Ser in *Am*VHPO, the halogen specificity cannot be traced back to a direct
171 interaction of a single amino acid residue with the halogen or the vanadate cofactor. Different
172 amino acids influence the oxidation potential towards chloride and/or accelerate the speed of
173 oxidation in the class of VHPO enzymes. Thus, a more systemic analysis of VHPOs is needed
174 to reveal the structure-activity relationship.



175

176 **Fig. 3 | Mutant screening and aromatic halogenations of phenol red (5).** a) Bromination and chlorination
 177 activities of relevant R425 mutants using monochlorodimedone (MCD, **3**) assay. The serine variant stands out with
 178 a ten times higher conversion of MCD (**3**) than the wild-type. Comparison of b) the aromatic bromination and c)
 179 aromatic chlorination ability over time using phenol red (**5**) and d) 1,3,5-trimethoxybenzene (**7**, TMB) using the wild-
 180 type AmVHPO and the variants R425D and R425S.

181

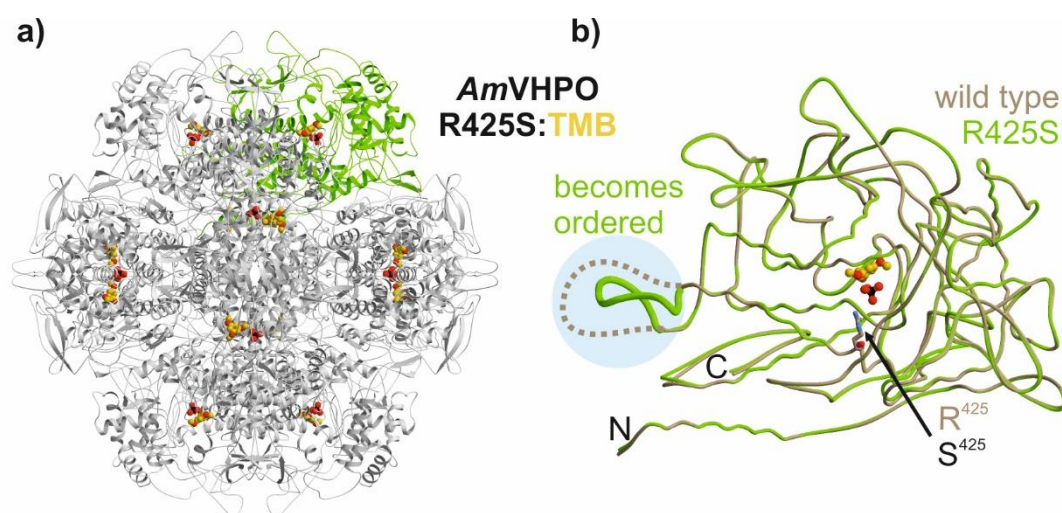
182 Additionally, alternative substrates were examined for enzymatic halogenations. The R425S
 183 mutant preferentially accepts aryl derivatives and thus exhibits a similar substrate scope as
 184 the wild-type enzyme. A comparison of our standard reaction with phenol red (**5**) revealed that

185 the R425S variant chlorinated both substrates. At the same time, no activity was measured in
186 the presence of the wild-type enzyme or the R425D mutant (Figure 3b). Intriguingly, a range
187 of other aromatic substrates, such as TMB (**7**), thymol indoles, pyridines. were transformed to
188 the corresponding chlorinated products with excellent regioselectivities and high yields (see
189 SI, chapter 10).

190

191 **Molecular insights into *Am*VHPO variants.** To understand the role of position 425 for
192 halogen specificity in *Am*VHPO, we crystallized each, a catalytically highly competent VCPO
193 (R425S, PDB ID 8Q21 and 8Q22; see SI, STable 5) and a VBPO (R425D, PDB ID 8Q20; see
194 SI, STable 5) mutant by the hanging drop vapor diffusion method. An isosteric phosphate,
195 obtained from the reservoir solution,^{6d} replaced the cofactor vanadate in the enzyme crystals.
196 Both mutant structures feature the identical characteristic assembly of a hexamer of dimers,
197 arranged in a 'head-to-tail' orientation with superimposable key catalytic residues when
198 compared to the wild-type (Fig. 4a). Remarkably, variant R425S showed an interaction
199 between Ser425 and a region of the adjacent subunit (Fig. 4b, highlighted in blue). In detail,
200 residues 390-404 in the wild-type structure lack a defined electron density due to flexibility. In
201 contrast, in R425S, this section consolidated in a loop structure, strongly influenced by the
202 introduced serine residue (Fig. 4b, highlighted in blue). The hypothesis that this loop is
203 responsible for the halogen specificity is supported by the crystal structure analyses of the
204 *Am*VHPO mutant R425D (cf. Fig. 5), which has no chlorination activity and lacks a structured
205 conformation of residues 400-405.

206



207

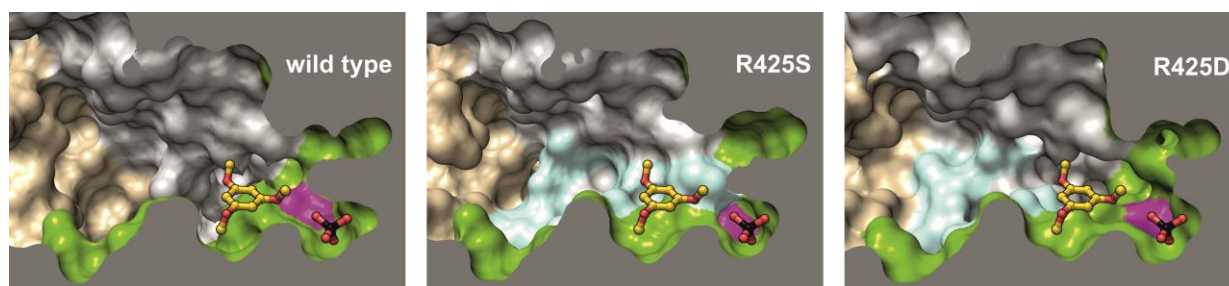
208 **Fig. 4 | X-ray structure of the *Am*VHPO-R425S mutant in complex with 1,3,5-trimethoxybenzene (**7**, TMB).** a)
209 Ribbon diagram of dodecameric *Am*VHPO-R425S mutant with its surrogate TMB (**7**, one subunit is depicted in
210 green, **7** and phosphate (PO₄³⁻) are shown as a ball-and-stick model with gold carbon atoms; PDB ID 8Q22). b)
211 Structural superposition of *Am*VHPO-R425S (green) and wild-type *Am*VHPO (tan, PDB ID 5LPC). Dots indicate a

212 loop region that lacks defined electron density in the wild-type structure (residues 390-404, highlighted in cyan) but
213 which adopts a defined motif in the mutant.

214

215 A long-standing hypothesis is that VHPO-catalyzed halogenation of organic compounds
216 occurs outside the enzyme, with the corresponding hypohalous acid diffusing freely in solution.
217 However, there is increasing evidence for a more complex mechanism within the catalytic
218 center of these enzymes.^{9,21} Recently, extensive investigations on the bacterial VCPOs
219 operating with high selectivity in the napyradiomycin and merochlorin biosynthesis^{11h} and
220 computational studies together with kinetic experiments on *CMHPO*¹⁰ hinted at a substrate
221 binding site in these VHPOs. This assumption aligns with earlier investigations demonstrating
222 that indoles and terpenes are preferentially brominated over MCD (**3**) when these substrates
223 are present in equimolar concentrations.^{10,13a} Despite these important studies, there is still a
224 massive debate on the existence of a substrate-binding site in VHPOs and whether the
225 halogenation occurs within the substrate enzyme complex or outside the enzyme by freely
226 diffusing HOX. However, for the highly reactive hypochlorous species HOCl, the chlorination
227 reaction likely occurs immediately after the in-situ formation of the electrophilic chlorine
228 reagent, rendering the halogenation of an enzyme-bound substrate very likely. Competition
229 assays for the chlorination of **3** in the presence of varying amounts of TMB (**7**) showed a
230 preference for TMB over **3** (see SI, chapter 6). The hypothesis of a substrate binding site in
231 R425S-*AmVHPO*s was thus further verified. Encouraged by this result, we started co-
232 crystallization experiments using **7** as a ligand. As shown in Figure 5, TMB (**7**) only binds to
233 the *AmVHPO* once the ordered loop region at the interface of two enzyme subunits (loop
234 region, residue 390-404, cyan) is defined. In the R425D mutant, this motif is only partially
235 present (residue 390-400), so no interactions with **7** can occur. These molecular findings agree
236 with the wild-type structure, in which residues 390-404 are also flexible. Thus, the plasticity of
237 the specificity pocket depends on the introduced mutant, and only a small modular sequence
238 motif coordinates substrate selection (Fig. 6a). Consequently, no substrate-binding site is
239 present in the wild-type *AmVHPO*.

240



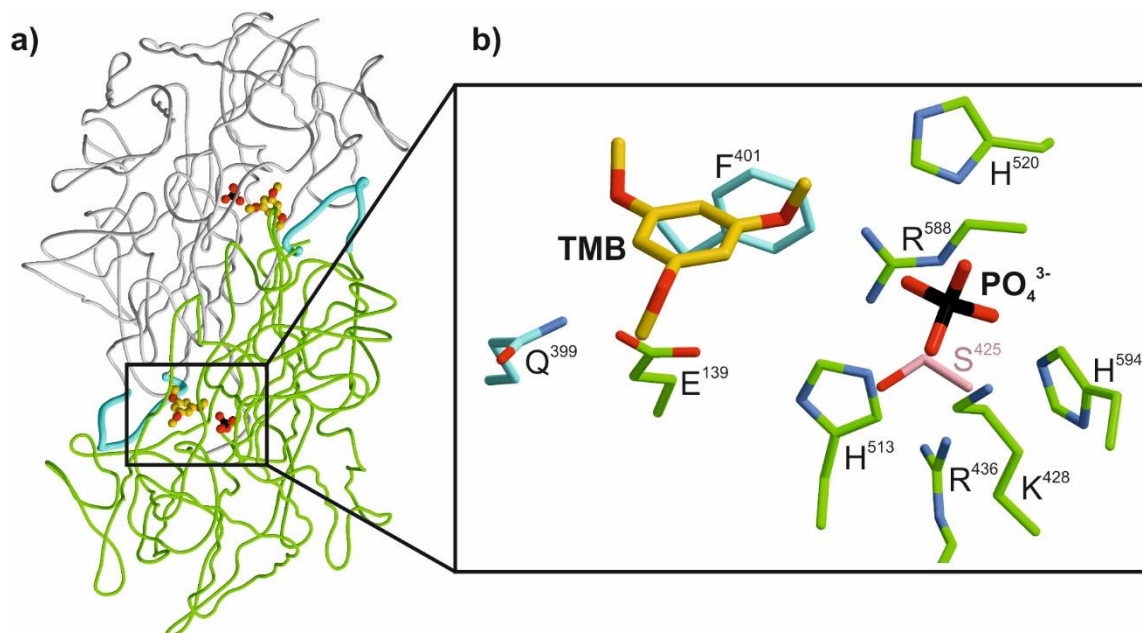
241 **Fig. 5 | Surface cross-section of *AmVHPO* variants in complex with 1,3,5-trimethoxybenzene (**7**).** The cartoon
242 represents one of 12 active sites in *AmVHPO*. The substrate binding pocket comprises two *AmVHPO* subunits
243 shown in green and grey, respectively. Other subunits of the dodecamer are colored brown. TMB (**7**) is only bound

244 in the R425S mutant (PDB ID 8Q22). Superposition of the liganded *Am*VHPO-R425S mutant with wild-type (PDB
245 ID 5LPC) and R425D (PDB ID 8Q20) structures illustrates how **7** may bind in these variants. Residue 425 (magenta)
246 has a significant impact on the shape of the specificity pocket: TMB (**7**) is stabilized by a defined loop region from
247 the adjacent subunit (residues 390-404, highlighted in cyan), which is fully resolved in R425S, flexible in the wild-
248 type structure and partially present in R425D.

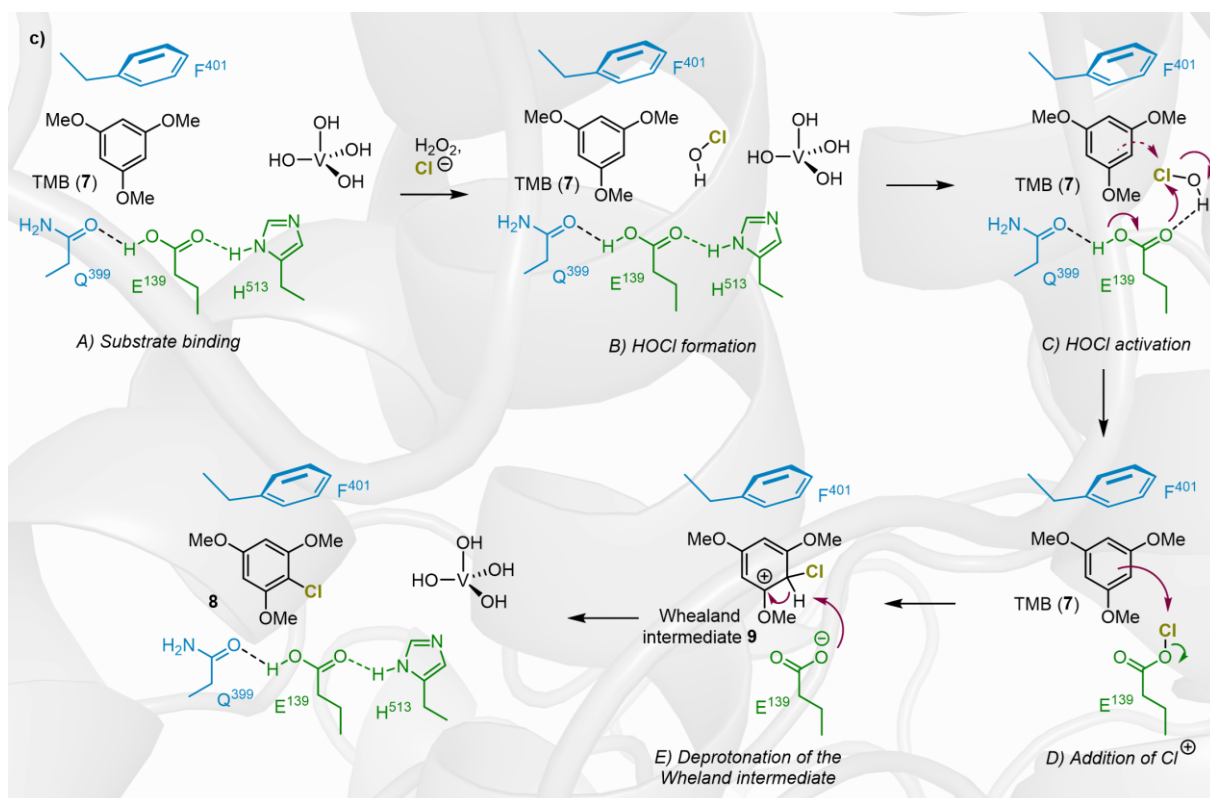
249

250 Figures 6a and 6b depict the protein residues surrounding TMB (**7**) in the substrate-R425S-
251 *Am*VHPO complex. These residues include Glu139 with Gln399 and Phe401 from the
252 neighboring subunit in proximity to the vanadate cofactor (replaced by phosphate in the X-ray
253 crystal structure). These amino acid side chains favor the anchoring of aromatic substrates. A
254 distance of 3.6 Å between Phe401 and TMB (**7**) indicates a strong π - π stacking that stabilizes
255 the aryl-moiety of **7**. Hydrogen bonding of Glu139 and Gln399 (2.8 Å) and their interaction with
256 the active site His513 facilitate the electrophilic aromatic chlorination (S_EAr). Taken together,
257 the combination of a narrowly shaped specific binding pocket that extends the residence time
258 of substrates near the active site, together with structural rearrangements forging a tunnel
259 structure at the interface of two neighboring subunits, enables chlorination reactions in our
260 engineered R425S-*Am*VHPO variant. These results are consistent with findings in flavin-
261 dependent halogenases in which tunnel formation can abolish HOX leakage, leading to
262 increased halogenation efficiency.²²

263 To shed light on the effects of Glu139 and Phe401 on the catalytic chlorination process, we
264 replaced each of these two amino acids with glycine, generating conformationally more flexible
265 double mutants R425S E139G and R425S F401G, respectively. Intriguingly, the chlorination
266 reaction no longer took place in the F401G mutant, as shown in the enzymatic activity and
267 halide specificity assays (see SI, SFig. 9), but was just slowed down for brominations (cf. SI,
268 SFig. 8). This hints at the binding of the aryl substrate being decisive for chlorinations but only
269 having minor effects on bromination reactions. The E139G variant, however, showed a
270 different behavior. A significant decrease in chlorination activity was indeed observed in the
271 MCD (**3**, conversion of **3** was decreased by 20% after 15 min) and in the phenol red assay. At
272 the same time, no bromination was detectable at all. Moreover, the chlorination of TMB (**7**)
273 was only detectable in traces according to GC analysis. This emphasizes the supporting
274 function of the carboxylic acid for delivering the electrophilic halide species HOX to the
275 substrate and its role in stabilizing the cationic Wheland intermediate **9** (Figure 6c).



276



277

278 **Fig. 6 | The active site in *AmVHPO* is formed by two adjacent subunits.** a) Coil representation of neighboring
 279 subunits in the *AmVHPO*: TMB-R425S complex. The phosphate mimicking the catalytic vanadate is coordinated by
 280 one subunit, while the substrate binding channel is formed together with the adjacent subunit. The loop region from
 281 the flanking subunit is crucial for TMB binding (loop region, residues 390-404, highlighted in cyan) and is structured
 282 only in the R425S mutant. b) Close-up view of the active site with protein side chains engaged in ligand and
 283 phosphate binding. S425 is colored pink. c) Proposed schematic mechanism of enzymatic chlorination in R425S-
 284 *AmVHPO*.

285

286 **Discussion.** Vanadium-dependent haloperoxidases (VHPOs) are, in principle, ideal enzymes
287 for applications in industrial processes as they are robust to organic synthetic reaction
288 conditions and need just simple halides together with H₂O₂ and vanadate to be operative. The
289 structural features responsible for halogen specificity are still elusive as the amino acids inside
290 the active site in VHPOs are highly conserved. Therefore, halide specificity must be controlled
291 around the vanadate binding site in the second or third sphere. The majority of identified
292 VHPOs produce short-lived, highly reactive hypohalites, which exhibit non-specific
293 halogenation reactivity towards diverse substrates.^{4a,23} In contrast, highly stereoselective
294 chlorofunctionalizations within the biosynthesis of napyradiomycins and merochlorins (cf. Fig.
295 1c) by VHPOs from marine *Streptomyces* are known.^{11a} This led to a highly controversial
296 discussion on the location of halogenation, inside or outside the enzyme.

297 Our study reveals that position 425 in *Am*VHPO, located i+3 from the active site Lys428, plays
298 an important role in halogen specificity and substrate binding. Exchanging Arg425 by serine
299 organizes residues 390-404 in R425S to a defined loop. This structural variation has no
300 immediate influence on its protein subunit but causes mutual interactions of two neighboring
301 monomers in the 'head-to-tail' orientation of the dodecameric enzyme structure.
302 Consequently, the loop triggers the formation of a defined tunnel with the vanadate cofactor at
303 the end. Within this tunnel, a combination of structure-induced interactions is observed to be
304 responsible for substrate halogenation. A compelling interplay of Glu139, His513, and Gln399
305 from the neighboring subunit near the active site was induced in the R425S-variant (Fig. 6).
306 Although the key catalytic residues in the first coordination sphere of cofactor binding are still
307 strictly conserved within the R425S-*Am*VHPO mutant, the Ser425 from the adjacent subunit
308 alters the hydrogen-bonding network within the active site, thus forming a tunnel protecting the
309 vanadate in the active site. This reduces the access of solvent molecules to the vanadate
310 cofactor and thus abolishes the degradation of the reactive Cl⁺ species. Such active sites with
311 hampered accessibility in VHPOs have been reported only in the structurally characterized
312 bacterial VCPOs, catalyzing stereoselective chlorofunctionalizations,^{11h} and the VHPO from
313 *Zobellia galactanivorans* (*Zg*VHPO).²⁴ Nevertheless, comparing the structures of the wild-type
314 VBPOs from *A. marina*, *C. officinalis*, and *C. pulifera* with those of VHPOs exhibiting
315 chlorination activity (*A. nodosum*, *C. inaequalis*, *Streptomyces CHN-189*) given the knowledge
316 gained in the presented study a significant correlation between the exposure of the vanadate
317 cofactor and their halogenation activity becomes obvious (cf. SI, chapter 9, SFig. 18) and
318 corroborates the conclusions drawn from our mutagenesis experiments. While the active site
319 vanadate is located at the end of a broad funnel in all VBPOs, ensuring fast substrate access
320 and release of the electrophilic HOX species, different tunnel structures toward the prosthetic
321 group are visible in all chlorinating VHPOs. In addition, a direct correlation between
322 halogenation activity and the extent of the tunnel is visual—the more shielded the cofactor, the

323 higher and more specific the chlorination activity. The same structure-reactivity relationship is
324 visible between the wild-type *Am*VHPO and the R425D and R425S mutants (cf. SI, chapter 9,
325 SFig. 20). The access to the active site in the native and the genetically altered enzymes forms
326 close to the interface between two protein subunits. The interaction between those monomers
327 is primarily determined by loop structures (cf. SI, chapter 9, SFigure 19). While in the wild-type
328 *Am*VHPO, the upper loop is not resolved, leaving broad access to the vanadate group, two
329 distinct loops in *Co*VHPO and *Cp*VHPO frame the active site entrance and form a wide and
330 surface-exposed funnel. In *An*VHPO, however, it is mainly the upper loop that engages in
331 tunnel formation in front of the active site, correlating with an onset of chlorination activity. This
332 loop is in the same region as the non-resolved loop in wt-*Am*VHPO that becomes ordered in
333 the R425S mutant, hinting at the influence of this structure on halogen selectivity. Also, in the
334 bacterial NapH1, two prominent loops in the respective N-terminal part of each subunit strongly
335 interact at the monomers' interface. They are responsible for the dense packing around the
336 active site. Only the chloroperoxidase *Cv*VHPO acts as a monomer but likewise uses a loop
337 structure in front of the active site that closes off the entrance and takes part in tunnel formation.
338 All these observations show that the defined loop formation and its induction to form a tunnel
339 structure to the active site is a general scheme in VHPOs that regulate substrate specificity
340 and reactivity. This further underlines the importance and broad application of our successful
341 engineering approach.

342 Furthermore, the structural rearrangement induced by the single point mutation led to a defined
343 specificity pocket inside the newly formed tunnel, enabling TMB (7) binding at the intersection
344 of two neighboring subunits. The released hypochlorous acid can now immediately react with
345 the substrate, thus further contributing to the enhanced chlorination ability of R425-*Am*VHPO.
346 The structural and biochemical studies highlight Phe401 and Glu139 as crucial residues for
347 substrate binding and halogenation activity, with a significant or even total activity loss upon
348 their exchange by glycine. Remarkably, glutamic acid also plays a dominant role in flavin-
349 dependent (FAD) halogenases and is crucial for high reaction rates.²⁵ For example, the single
350 point mutation E346Q in the flavine-dependent halogenase PrnA caused a reduction in
351 halogenation rate by two orders of magnitude.²⁶ Theoretical investigations and active site
352 mutagenesis studies showed that localization of negative charge and the interaction with the
353 chlorinating species is essential for the electrophilic aromatic substitution in such enzymes. In
354 our R425S variant, the hypochloric acid formed at the vanadate cofactor coordinates to Glu139
355 via hydrogen bonding, thus shuttling Cl⁺ from the vanadate binding site to the substrate binding
356 site. Simultaneously, Glu139 increases the electrophilicity by this hydrogen-bonding interaction
357 or even by forming the glutamyl hypochlorite intermediate (D, Figure 6c). Both activation
358 modes will lead to an electrophilic addition of the aromatic ring to the corresponding hypohalite
359 species (dashed versus plain arrows). It is plausible that the E139G variant could not chlorinate

360 TMB (**7**) due to lower electronic activation of the substrate compared to **3** and **5** (see SI, chapter
361 4). After the electrophilic Cl⁺ is transferred to TMB (**7**), Glu139 stabilizes the cationic Wheland
362 intermediate (**9**, Figure 6c) via ionic interactions, and the carboxylate moiety in Glu139
363 facilitates deprotonation of cationic intermediate furnishing the final product **8**.

364 In summary, our results provide insights into the long-standing question of halogen specificity
365 in VHPOs and have proven the existence of a substrate-binding site in VHPOs for the first
366 time. An AI-guided rational design led to a successful enzyme engineering to switch the
367 halogen specificity in *Am*VHPOs. A single point mutation of an amino acid residue outside the
368 active site (position 425) in *Am*VHPO initiates a complex structural rearrangement within the
369 protein scaffold, leading to an engineered enzyme pocket, which enables efficient aromatic
370 chlorinations. Comparing the structures of different VHPOs points toward a general correlation
371 between the chloroperoxidase activity and the enclosure of the active site prosthetic group
372 within the enzyme, which is influenced by loops surrounding the entrance to the active site that
373 is mainly located at the interface of two neighboring protein subunits. Halogen oxidation and
374 halogen delivery in VHPOs are locally separated and occur at different binding sites that are
375 closely related. While the vanadate binding site is responsible for halogen oxidation, another
376 binding site in the surroundings accommodates a specific substrate. In addition, a glutamic
377 acid residue within the substrate binding site plays a decisive role in the chlorination ability of
378 aromatic substrates. These structural features are similar to those identified in FAD-dependent
379 halogenases and corroborate a similar concept applied by nature for selective halogenations
380 in both enzyme classes. Given the advantages of VHPOs for organic synthesis compared to
381 classical chemical catalysts, especially regarding sustainability and environmental protection,
382 we are convinced that our findings will lay the foundation for their further engineering and, thus,
383 biotechnological application in the future.

384 **Acknowledgments**

385 We thank Prof. T.A.M. Gulder for the fruitful discussions. This work was funded by the Emmy-
386 Noether and Heisenberg program of the German Research Foundation (DFG, GU 1134/3-1
387 and GU 1134/4). C.J.S. thanks the Deutsche Bundesstiftung Umwelt for a fellowship (grant
388 20015/400).

389

390 **Data availability**

391 The authors declare that the data supporting the findings of this study are available within the
392 paper and its supplementary information files or can be obtained from the corresponding author
393 on reasonable request. The Rosetta software suite used for structure preparation and ddG
394 calculations is publicly available under the RosettaCommons license. Specific scripts for the

395 computational pipeline in this publication can be accessed at
396 <https://github.com/ClaraTSchoeder/schoederlab> and are given in Supplementary Data 1. In
397 addition, the protein X-ray crystal structures have been deposited at the Protein Data Bank
398 under the following accession codes: 5LPC (wild-type *Am*VHPO), 8Q20 (*Am*VHPO R425D
399 mutant), 8Q21 (*Am*VHPO R425S mutant), 8Q22 (*Am*VHPO R425S mutant with TMB).

400

401 References

- 402 1 Crowe, C., Molyneux, S., Sharma, S. V., Zhang, Y., Gkotsi, D. S., Connaris, H. & Goss, R. J. M.
403 Halogenases: a palette of emerging opportunities for synthetic biology–synthetic chemistry
404 and C–H functionalization. *Chem. Soc. Rev.* **50**, 9443–9481, doi:10.1039/D0CS01551B (2021).
- 405 2 Saikia, I., Borah, A. J. & Phukan, P. Use of Bromine and Bromo-Organic Compounds in Organic
406 Synthesis. *Chemical Reviews* **116**, 6837–7042, doi:10.1021/acs.chemrev.5b00400 (2016).
- 407 3 a) Gribble, G. W. Natural Organohalogens: A New Frontier for Medicinal Agents? *J. Chem. Educ.*
408 **81**, 1441–1449 (2004), b) Gribble, G. W. The Diversity of Naturally Produced
409 Organohalogens. *Chemosphere* **52**, 289–297 (2003), c) Gribble, G. W. Naturally Occurring
410 Organohalogen Compounds. *Acc. Chem. Res.* **31**, 141–152 (1998), d) Wagner, C., El Omari,
411 M. & König, G. M. Biohalogenation: Nature’s Way to Synthesize Halogenated Metabolites
412 *J. Nat. Prod.* **72**, 540–553 (2009), e) Paul, C. & Pohnert, G. Production and role of volatile
413 halogenated compounds from marine algae. *Nat. Prod. Rep.* **28**, 186–195,
414 doi:10.1039/c0np00043d (2011), f) Gribble, G. W. Naturally Occurring Organohalogen
415 Compounds—A Comprehensive Review. *Prog. Chem. Org. Nat. Prod.* **121**, 1–546,
416 doi:10.1007/978-3-031-26629-4_1 (2023).
- 417 4 a) Butler, A. & Sandy, M. Mechanistic Considerations of Halogenating Enzymes. *Nature* **460**, 848
418 (2009), b) Agarwal, V., Miles, Z. D., Winter, J. M., Eustáquio, A. S., El Gamal, A. A. &
419 Moore, B. S. Enzymatic halogenation and dehalogenation reactions: pervasive and
420 mechanistically diverse. *Chemical reviews* **117**, 5619–5674 (2017).
- 421 5 a) Hanefeld, U., Hollmann, F. & Paul, C. E. Biocatalysis making waves in organic chemistry. *Chem.*
422 *Soc. Rev.* **51**, 594–627, doi:10.1039/D1CS00100K (2022), b) Höfler, G. T., But, A. &
423 Hollmann, F. Haloperoxidases as catalysts in organic synthesis. *Org. Biomol. Chem.* **17**, 9267–
424 9274, doi:10.1039/C9OB01884K (2019), c) Wu, S., Snajdrova, R., Moore, J. C., Baldenius,
425 K. & Bornscheuer, U. T. Biocatalysis: Enzymatic Synthesis for Industrial Applications. *Angew.*
426 *Chem. Int. Ed.* **60**, 88–119, doi:<https://doi.org/10.1002/anie.202006648> (2021), d)
427 Truppo, M. D. Biocatalysis in the Pharmaceutical Industry: The Need for Speed. *ACS*
428 *Medicinal Chemistry Letters* **8**, 476–480, doi:10.1021/acsmedchemlett.7b00114 (2017), e)
429 France, S. P., Lewis, R. D. & Martinez, C. A. The Evolving Nature of Biocatalysis in
430 Pharmaceutical Research and Development. *JACS Au* **3**, 715–735, doi:10.1021/jacsau.2c00712
431 (2023).
- 432 6 a) van Schijndel, J. W. P. M., Barnett, P., Roelse, J., Vollenbroek, E. G. M. & Wever, R. The Stability
433 and Steady-State Kinetics of Vanadium Chloroperoxidase from the Fungus *Curvularia*
434 *inaequalis*. *Eur. J. Biochem.* **225**, 151 (1994), b) Tromp, M. G. M., olafsson, G., Krenn,
435 B. E. & Wever, R. Some structural aspects of vanadium bromoperoxidase from *Ascophyllum*
436 *nodosum*. *Biochim. Biophys. Act.* **1040**, 192–198, doi:[https://doi.org/10.1016/0167-4838\(90\)90075-Q](https://doi.org/10.1016/0167-4838(90)90075-Q) (1990), c) de Boer, E., Plat, H., Tromp, M. G. M., Wever, R., Franssen, M.
437 C. R., van der Plas, H. C., Meijer, E. M. & Schoemaker, H. E. Vanadium containing
438 bromoperoxidase: An example of an oxidoreductase with high operational stability in aqueous
439 and organic media. *Biotech. Bioengin.* **30**, 607–610,
440 doi:<https://doi.org/10.1002/bit.260300504> (1987), d) Frank, A., Seel, C. J., Groll, M. &
441 Gulder, T. Characterization of a cyanobacterial haloperoxidase and evaluation of its
442

- 443 biocatalytic halogenation potential. *ChemBioChem* **17**, 2028-2032,
444 doi:10.1002/cbic.201600417 (2016).
- 445 7 Seel, C. J. & Gulder, T. Biocatalysis Fueled by Light: On the Versatile Combination of
446 Photocatalysis and Enzymes. *ChemBioChem* **20**, 1871-1897, doi:10.1002/cbic.201800806
447 (2019).
- 448 8 a) Agarwal, V., Miles, Z. D., Winter, J. M., Eustáquio, A. S., El Gamal, A. A. & Moore, B. S. Enzymatic
449 halogenation and dehalogenation reactions: pervasive and mechanistically diverse. *Chem. Rev.*
450 **117**, 5619 (2017), b) Chen, Z. Recent Development of Biomimetic Halogenation Inspired by
451 Vanadium Dependent Haloperoxidase. *Coord. Chem. Rev.* **457**, 214404 (2022).
- 452 9 Hemrika, W., Renirie, R., Macedo-Ribeiro, S., Messerschmidt, A. & Wever, R. Heterologous
453 Expression of the Vanadium-containing Chloroperoxidase from *Curvularia inaequalis* in
454 *Saccharomyces cerevisiae* and Site-directed Mutagenesis of the Active Site Residues His⁴⁹⁶,
455 Lys³⁵³, Arg³⁶⁰, and Arg⁴⁹⁰. *Journal of Biological Chemistry* **274**, 23820-23827,
456 doi:10.1074/jbc.274.34.23820 (1999).
- 457 10 Gérard, E. F., Mokkaes, T., Johannissen, L. O., Warwicker, J., Spiess, R. R., Blanford, C. F., Hay,
458 S., Heyes, D. J. & de Visser, S. P. How Is Substrate Halogenation Triggered by the Vanadium
459 Haloperoxidase from *Curvularia inaequalis*? *ACS Catal.* **13**, 8247-8261,
460 doi:10.1021/acscatal.3c00761 (2023).
- 461 11 a) Murray, L. A. M., McKinnie, S. M. K., Moore, B. S. & George, J. H. Meroterpenoid natural
462 products from *Streptomyces* bacteria - the evolution of chemoenzymatic syntheses. *Nat. Prod.*
463 *Rep.* **37**, 1334 (2020), b) Miles, Z. D., Diethelm, S., Pepper, H. P., Huang, D. M., George,
464 J. H. & Moore, B. S. A unifying paradigm for naphthoquinone-based meroterpenoid
465 (bio)synthesis. *Nat. Chem.* **9**, 1235 (2017), c) Teufel, R., Kaysser, L., Villaume, M. T.,
466 Diethelm, S., Carbullido, M. K., Baran, P. S. & Moore, B. S. One-pot enzymatic synthesis of
467 merochlorin A and B. *Angew. Chem., Int. Ed.* **53**, 11019 (2014), d) Diethelm, S., Teufel,
468 R., Kaysser, L. & Moore, B. S. A multitasking vanadium-dependent chloroperoxidase as an
469 inspiration for the chemical synthesis of the merochlorins. *Angew. Chem., Int. Ed.* **53**, 11023
470 (2014), e) Kaysser, L., Bernhardt, P., Nam, S. J., Loesgen, S., Ruby, J. G., Skewes-Cox, P.,
471 Jensen, P. R., Fenical, W. & Moore, B. S. Merochlorins A-D, cyclic meroterpenoid antibiotics
472 biosynthesized in divergent pathways with vanadium-dependent chloroperoxidases. *J. Am.*
473 *Chem. Soc.* **134**, 11988 (2012), f) Bernhardt, P., Okino, T., Winter, J. M., Miyanaga, A. &
474 Moore, B. S. A stereoselective vanadium-dependent chloroperoxidase in bacterial antibiotic
475 biosynthesis. *J. Am. Chem. Soc.* **133**, 4268 (2011), g) Winter, J. M. & Moore, B. S. Exploring
476 the chemistry and biology of vanadium-dependent haloperoxidases. *J. Biol. Chem.* **284**, 18577
477 (2009), h) Chen, P. Y.-T., Adak, S., Chekan, J. R., Liscombe, D. K., Miyanaga, A., Bernhardt,
478 P., Diethelm, S., Fielding, E. N., George, J. H., Miles, Z. D., Murray, L. A. M., Steele, T. S., Winter,
479 J. M., Noel, J. P. & Moore, B. S. Structural Basis of Stereospecific Vanadium-Dependent
480 Haloperoxidase Family Enzymes in Napyradiomycin Biosynthesis. *Biochemistry* **61**, 1844-1852,
481 doi:10.1021/acs.biochem.2c00338 (2022), i) McKinnie, S. M. K., Miles, Z. D., Jordan, P. A.,
482 Awakawa, T., Pepper, H. P., Murray, L. A. M., George, J. H. & Moore, B. S. Total enzyme
483 syntheses of napyradiomycins A1 and B1. *J. Am. Chem. Soc.* **140**, 17840 (2018).
- 484 12 Messerschmidt, A. & Wever, R. X-ray structure of a vanadium-containing enzyme:
485 chloroperoxidase from the fungus *Curvularia inaequalis*. *Proc. Natl. Acad. Sci. U. S. A.* **93**, 392
486 (1996).
- 487 13 a) Carter-Franklin, J. N., Parrish, J. D., Tschirret-Guth, R. A., Little, R. D. & Butler, A. Vanadium
488 Haloperoxidase-Catalyzed Bromination and Cyclization of Terpenes. *J. Am. Chem. Soc.* **125**,
489 3688 (2003), b) Carter-Franklin, J. N. & Butler, A. Vanadium Bromoperoxidase-
490 Catalyzed Biosynthesis of Halogenated Marine Natural Products. *J. Am. Chem. Soc.* **126**, 15060
491 (2004).
- 492 14 Markus, B., C, G. C., Andreas, K., Arkadij, K., Stefan, L., Gustav, O., Elina, S. & Radka, S.
493 Accelerating Biocatalysis Discovery with Machine Learning: A Paradigm Shift in Enzyme
494 Engineering, Discovery, and Design. *ACS Catal.*, 14454-14469, doi:10.1021/acscatal.3c03417
495 (2023).

- 496 15 a) Seel, C. J., Kralik, A., Hacker, M., Frank, A., Koenig, B. & Gulder, T. Atom-Economic Electron
497 Donors for Photobiocatalytic Halogenations. *ChemCatChem* **10**, 3960-3963,
498 doi:10.1002/cctc.201800886 (2018), b) Wells, C. E., Ramos, L. P. T., Harstad, L. J.,
499 Hessefort, L. Z., Lee, H. J., Sharma, M. & Biegasiewicz, K. F. Decarboxylative Bromooxidation of
500 Indoles by a Vanadium Haloperoxidase. *ACS Catal.* **13**, 4622-4628,
501 doi:10.1021/acscatal.2c05531 (2023).
- 502 16 Dauparas, J., Anishchenko, I., Bennett, N., Bai, H., Ragotte, R. J., Milles, L. F., Wicky, B. I. M.,
503 Courbet, A., de Haas, R. J., Bethel, N., Leung, P. J. Y., Huddy, T. F., Pellock, S., Tischer, D., Chan,
504 F., Koepnick, B., Nguyen, H., Kang, A., Sankaran, B., Bera, A. K., King, N. P. & Baker, D. Robust
505 deep learning-based protein sequence design using ProteinMPNN. *Science* **378**, 49-56,
506 doi:10.1126/science.add2187 (2022).
- 507 17 Ohshiro, T., Littlechild, J., Garcia-Rodriguez, E., Isupov, M. N., Iida, Y., Kobayashi, T. & Izumi, Y.
508 Modification of halogen specificity of a vanadium-dependent bromoperoxidase. *Protein Sci.*
509 **13**, 1566-1571, doi:<https://doi.org/10.1110/ps.03496004> (2004).
- 510 18 a) Barlow, K. A., Ó Conchúir, S., Thompson, S., Suresh, P., Lucas, J. E., Heinonen, M. & Kortemme,
511 T. Flex ddG: Rosetta Ensemble-Based Estimation of Changes in Protein-Protein Binding Affinity
512 upon Mutation. *J. Phys. Chem. B* **122**, 5389-5399, doi:10.1021/acs.jpbc.7b11367 (2018), b)
513 Park H Fau - Bradley, P., Bradley, P., Greisen P Jr Fau - Liu, Y., Liu Y Fau - Mulligan, V. K.,
514 Mulligan Vk Fau - Kim, D. E., Kim De Fau - Baker, D., Baker D Fau - DiMaio, F. & DiMaio, F.
515 Simultaneous Optimization of Biomolecular Energy Functions on Features from Small
516 Molecules and Macromolecules. *J. Chem. Theory Comput.* **12**, 6201-6212, doi:
517 10.1021/acs.jctc.6b00819 (2016).
- 518 19 a) Hager, L. P., Morris, D. R., Brown, F. S. & Eberwein, H. Chloroperoxidase. *J. Biol. Chem.* **241**,
519 1769 (1966), b) Verhaeghe, E., Buisson, D., Zekri, E., Leblanc, C., Potin, P. & Ambroise,
520 Y. A Colorimetric Assay for Steady-State Analyses of Iodo- and Bromoperoxidase Activities.
521 *Analyt. Biochem.* **379**, 60 (2008).
- 522 20 Cochereau, B., Le Strat, Y., Ji, Q., Pawtowski, A., Delage, L., Weill, A., Mazéas, L., Hervé, C.,
523 Burgaud, G., Gunde-Cimerman, N., Pouchus, Y. F., Demont-Caulet, N., Roullier, C. & Meslet-
524 Cladiere, L. Heterologous Expression and Biochemical Characterization of a New
525 Chloroperoxidase Isolated from the Deep-Sea Hydrothermal Vent Black Yeast *Hortaea*
526 *werneckii* UBOCC-A-208029. *Mar. Biotechnol.*, doi:10.1007/s10126-023-10222-7 (2023).
- 527 21 a) Martinez, J. S., Carroll, G. L., Tschirret-Guth, R. A., Altenhoff, G., Little, R. D. & Butler, A. On the
528 Regiospecificity of Vanadium Bromoperoxidase. *J. Am. Chem. Soc.* **123**, 3289 (2001), b)
529 Littlechild, J., Garcia Rodriguez, E. & Isupov, M. Vanadium containing bromoperoxidase
530 – Insights into the enzymatic mechanism using X-ray crystallography. *Journal of Inorganic*
531 *Biochemistry* **103**, 617-621, doi:<https://doi.org/10.1016/j.jinorgbio.2009.01.011> (2009).
- 532 22 Prakinee, K., Phintha, A., Visitsatthawong, S., Lawan, N., Sucharitakul, J., Kantiwiriyanitch,
533 C., Damborsky, J., Chitnumsub, P., van Pée, K.-H. & Chaiyen, P. Mechanism-guided tunnel
534 engineering to increase the efficiency of a flavin-dependent halogenase. *Nat. Catal.* **5**, 534-
535 544, doi:10.1038/s41929-022-00800-8 (2022).
- 536 23 Leblanc, C., Vilter, H., Fournier, J. B., Delage, L., Potin, P., Rebuffet, E., Michel, G., Solari, P. L.,
537 Feiters, M. C. & Czjzek, M. Vanadium haloperoxidases: from the discovery 30 years ago to X-
538 ray crystallographic and V K-edge absorption spectroscopic studies. *Coord. Chem. Rev.* **301-
539 302**, 134 (2015).
- 540 24 Fournier, J. B., Rebuffet, E., Delage, L., Grijol, R., Meslet-Cladière, L., Rzonca, J., Potin, P.,
541 Michel, G., Czjzek, M. & Leblanc, C. The Vanadium Iodoperoxidase from the marine
542 flavobacteriaceae species *Zobellia galactanivorans* reveals novel molecular and evolutionary
543 features of halide specificity in the vanadium haloperoxidase enzyme family. *Appl. Environ.*
544 *Microbiol.* **80**, 7561 (2014).
- 545 25 a) Weichold, V., Milbredt, D. & van Pée, K.-H. Specific Enzymatic Halogenation—From the
546 Discovery of Halogenated Enzymes to Their Applications In Vitro and In Vivo. *Angew. Chem.*
547 *Int. Ed.* **55**, 6374-6389, doi:<https://doi.org/10.1002/anie.201509573> (2016), b)
548 Barker, R. D., Yu, Y., De Maria, L., Johannissen, L. O. & Scrutton, N. S. Mechanism of

549 Action of Flavin-Dependent Halogenases. *ACS Catal.* **12**, 15352-15360,
550 doi:10.1021/acscatal.2c05231 (2022).
551 26 a) Dong, C., Flecks, S., Unversucht, S., Haupt, C., van Pée, K.-H. & Naismith, J. H. Tryptophan 7-
552 Halogenase (PrnA) Structure Suggests a Mechanism for Regioselective Chlorination. *Science*
553 **309**, 2216-2219, doi:10.1126/science.1116510 (2005), b) Flecks, S., Patallo, E. P., Zhu,
554 X., Ernyei, A. J., Seifert, G., Schneider, A., Dong, C., Naismith, J. H. & van Pée, K.-H. New Insights
555 into the Mechanism of Enzymatic Chlorination of Tryptophan. *Angew. Chem. Int. Ed.* **47**, 9533-
556 9536, doi:<https://doi.org/10.1002/anie.200802466> (2008).
557